The object of this study is high-strength steel of API 5DP Gr 105 that has been used during well completion in a corrosive environment. This work emphasizes key factors affecting material damage caused by slip marks, tensile load, and hydrogen content in contaminated brine and completion fluid, which were not addressed in previous studies. Several tests, including chemical, mechanical, and surface characterization, were conducted. The chemical composition test of the fluid shows that the brine has been contaminated by H_2S gas and sulfur, with inevitable traces of chloride, bicarbonate, carbonate, bisulfide, and sulfide, providing active sites for hydrogen atom diffusion at the slip marks. The material composition test confirms that the failed material is API 5DP Gr 105. A noticeable amount of phosphorus increases grain boundary segregation and weakens the cohesive metallic bond. A hardness at 28 Rockwell C is inevitable and increases the material's vulnerability to embrittlement, despite the Charpy energy test showing a manageable level, confirming local brittleness. The high tensile strength of 914 MPa is evidence of embrittlement, even though the material remains ductile, with a noticeable elongation of 20%. An intergranular crack was observed in the microstructure, and slip marks serve as stress concentrators for the crack. Thus, it can be concluded that the combination of tensile load, hydrogen gas content, local slip marks, and completion fluid in the well weakened the grain boundaries and served as an initial crack with a high hydrogen-atom concentration. This work models the root-cause analysis of high-strength steel during well-completion operations in an onshore facility

Keywords: high-density completion fluid, hydrogen embrittlement, high-strength steel failure analysis, drilling completion

UDC 622.24:620.193.46:620.178
DOI: 10.15587/1729-4061.2026.361514

THE IDENTIFICATION OF HYDROGEN EMBRITTLEMENT AND THE ROLE OF INTERGRANULAR BRITTLE FRACTURE OF API 5DP G105 DRILL PIPE FAILURE ON ONSHORE DRILLING ACTIVITY

Sidhi Aribowo
PhD Student*
ORCID: https://orcid.org/0000-0002-7255-1931
Johny Wahyuadi Soedarsono
Corresponding author
Doctor of Engineering, Professor
Prof Johny Wahyuadi Laboratory*
E-mail: jwsono@metal.ui.ac.id
ORCID: https://orcid.org/0000-0001-6051-2866
Rini Riastuti
Doctor of Engineering, Professor
Prof Johny Wahyuadi Laboratory*
ORCID: https://orcid.org/0000-0003-3431-0413
Suryadi
Head of Engineering Services Division
Center for Materials Processing and Failure Analysis (CMPFA)*
ORCID: https://orcid.org/0000-0003-2739-7530
Slamet Nurhadi
Maintenance Manager**
ORCID: https://orcid.org/0009-0008-4361-1414
Warneri
Manager Rig Operation V**
ORCID: https://orcid.org/0009-0005-8552-1634
Sopar Mangarapot Simanullang
Assistant Manager Quality Control**
ORCID: https://orcid.org/0009-0005-6551-4816
Agus Kaban
Master of Engineering, Graduate Student
Prof Johny Wahyuadi Laboratory*
ORCID: https://orcid.org/0000-0002-9706-0506
Raajwa Ayudhia Kamila
Research Assistant
Prof Johny Wahyuadi Laboratory*
ORCID: https://orcid.org/0009-0003-4501-6647
*Department of Materials and Metallurgical Engineering
Universitas Indonesia
Kampus Baru UI Depok, Jawa Barat, Indonesia, 16424
**Pertamina Drilling Services Indonesia
MCC Building, Kuningan, Jakarta, Indonesia, 13140

Received 30.03.2026
Received in revised form 09.06.2026
Accepted 18.06.2026
Published 30.06.2026

How to Cite: *Aribowo, S., Soedarsono, J. W., Riasuti, R., Suryadi, Nurhadi, S., Warneri, Simanullang, S. M., Kaban, A. P. S., Kamila, R. A. (2026). The identification of hydrogen embrittlement and the role of intergranular brittle fracture of API 5DP G105 drill pipe failure on onshore drilling activity. Eastern-European Journal of Enterprise Technologies, 3 (1 (141)), 53–63. https://doi.org/10.15587/1729-4061.2026.361514*

1. Introduction

The oil and gas industry relies heavily on upstream operations to supply energy, with discovering productive wells being vital to meet ongoing energy demands. The escalate fossil fuel demand allows oil and gas operators to harness the optimization of drilling process as pivotal pathway for establishing and accelerating source of energy [1]. As an indispensable tool for transporting hydrocarbon drill pipes shows a promising way to meet delivery of source of energy to

surface facility processing unit while a good balance between maintenance and reliability is critical especially in offshore facility [2]. In this context, the mechanical integrity and properties of drill pipes are essential for navigating drilling challenges while ensuring safe operations. Although drilling pipes are considered the safest and most efficient means of delivering bulk energy, they are vulnerable to environmental degradation caused by exposure to corrosive conditions, applied stresses, and residual stresses.

The widespread use of high-strength steel for drilling pipes – primarily for transporting hydrocarbons from deep wells to surface facilities – makes this material both crucial and cost-effective for the hydrocarbon industry [3]. This steel's appealing mechanical properties, including excellent fatigue and corrosion resistance, are highly suitable for extended-reach drilling due to its controlled microstructure [4]. In this instance, recent industrial advancements often strike a good balance between mechanical performance and material resistance. However, the drawback of utilizing high-strength steel is attributed to the susceptibility of the material against dissipation of hydrogen into high-strength material. For instance, when exposed to hydrogen-rich well environments, drill pipes may suffer from hydrogen embrittlement (HE), which can lead to sudden fracture. Defects such as dislocations, grain boundaries, and secondary phases serve as pathways for hydrogen permeation. Accumulation of hydrogen at these sites can initiate cracks, reduce ductility, increase brittleness, and ultimately lead to material failure [5]. Controlling hydrogen absorption – either by reducing hydrogen uptake or enabling its diffusion out of the steel lattice – is vital for preventing such failures HE.

HE is recognized as the diffusion of hydrogen into the steel matrix, which reduces the ductility of the carbon steel. It is noteworthy that high-pressure hydrogen facilitates hydrogen penetration and embrittlement. Diffusible hydrogen reduces material elongation and reduction area, especially in the welded and heat-affected zones, due to thermal cycling, which changes their microstructure and affects mechanical properties. The susceptible material, hydrogen concentration, strength or hardness level, microstructure, HE sensitivity, residual stress and/or applied stress, and the embrittling and cracking temperature range are several critical factors of HE [6]. The other studies indicated that hydrogen trapping is gathered in lath interfaces, dislocation, including at the grain boundary of austenitic at lower energy sites [7].

In this context, the advancement of materials, including high-strength alloys, remains hindered by concerns about mechanical integrity in wet H2S environments rich in hydrogen [8]. HE poses non-permittable challenges to mechanical integrity, especially for drilling pipe, where exposure to wet H2S is inevitable, while structural reliability remains paramount. Several publications have extensively studied the effects of hydrogen penetration on various affected materials, including carbon steel, low-alloy steel, 400 SS, and high-strength steel.

Therefore, study devoted to the development of unveiling the effect of hydrogen diffusion in high-strength steel of metal such as API 5DP is relevant.

2. Literary review and problem statement

HE is inevitably present when hydrogen atoms penetrate the steel matrix before accumulating at various microstructural defects. HE occurs under multiple conditions, including the alloy material, service environment, stress, and strain. For example, the paper of [9] shows that austenitic stainless steel 304 remains susceptible to deformation due to hydrogen diffusion. The paper further reports that hydrogen charging causes pre-straining before deepening hydrogen dissipation, resulting from cross-linear deformation of alpha martensite. The report of [10] elaborates on the relationship between hydrogen entry and embrittlement, which is primarily due to the concentration of hydrogen that induces corrosion and accelerates it. The report emphasizes a strategy to maintain a critical hydrogen concentration below that on the surface of high-strength steel to hinder crack propagation. In addition, the paper [11] presents the results on increasing the HE resistance through the implementation of the thermomechanical method. In this case, the study employs the dual-phase heterostructure to improve the material's resistance to HE, making it a promising candidate for martensitic steel with elevated tensile strength.

But there were unresolved issues related to the prime reason for hydrogen embrittlement, such as the stress concentrator caused by the drill pipe defect. It is noteworthy to remember that drill pipe encounters loading of tension, torsion, pressure, bending, and cyclic fatigue, and further proceeds the geometrical or material discontinuity. The result of [12] demonstrates that sensitization and hydrogen charging on the austenitic stainless steel 304 and leads to hydrogen entrapment to reduce the tensile strength and elongation of material by nearly 10% and 17%. Further, the study reports that the presence of martensitic facilitates the transportation of hydrogen and localized the strain before conclude that the chromium control becomes a critical factor to hinder embrittlement.

The other elaborative publication of [13] observes the damage behavior of the high-strength steels with high composition of Mn and Al while maintaining the austenitic and ferritic volume. The study shows that decohesion, hydrogen-related, and local plasticity become the critical factors towards the failure, where the crack appears in the vicinity of the ferrite microstructure.

The paper [14] investigates macro- and microscale approaches to gain a deeper understanding of the impact of hydrogen on the reduction in the yield strength and ultimate tensile strength of X70 pipeline steel. The result shows that the inclusion of MnS and Al_2O_3, and the fracture features such as ductile dimples, are due to hydrogen charging of the steel microstructure. Particular attention is given to the result of [15], which distills the report that the high-density completion fluids (HDCF) where the pH, viscosity, and thermal stability are amongst the essential parameters of the solid-free HDCF. However, the study is challenging because slip marks, which act as stress concentrations, reduce the ductility of the API 5DP material during flexing.

A way to overcome these difficulties can be the implementation of visual inspection and surface and subsurface characterization. This approach was used in [16] to present the novel work to elaborate on the fatigue identification on the drill pipe at the various environmental factors on G105, S135, V150, and Ti alloy. The hardness and tensile test were utilized and showed the fatigue life can be prolonged based on the material selection process by choosing the Ti-based alloy as drill pipe in the mud drilling environment. However, the work to unveil the dissipation of hydrogen due to poor chemical injection of chemicals, H_2S contamination, sulfur decomposition, and material defect on API 5DP remains in siloes. The present work also focus on the relationship between the H_2S thermal dissociation of corrosion inhibitor based on thiocyanate to inhibit the sodium bromide excessive solution environment.

All this suggest that it is advisable to conduct a study on their damage mechanism and provide a future operational and material selection recommendation to hinder repetitive events that decrease the operational efficiency and unprecedented and unplanned shutdown.

3. The aim and objectives of the study

The aim of this study is to identifying the root cause of failure of API 5DP drill pipe material when it is used during the flexing/well completion process.

To achieve this aim, the following objectives were accomplished:

– to conduct the well fluid HDCF sample analysis including the material composition test through application of optical emission spectrometry (OES);

– to conduct the hardness test to evaluate the increasing of hardness due to the diffusion of hydrogen;

– to verify the material toughness and mechanical properties of the failed material to justify the root cause of failure through implementation of Charpy impact and tensile test;

– to assess the crack surface area through metallography, macro-structure, and microstructure.

4. Materials and methods

4. 1. The object and hypothesis of the study

The object of the study is API 5DP Gr 105 and categorized as a high-strength material where it heavily utilized as drill pipe to transport hydrocarbon from the well to the surface facilities equipment. The material was identified with a crack, where hydrogen diffusion is predicted to facilitate further fracture of the failed material. The assumption made in the study is based on the appearance of slip marks on the various locations of external failed pipe surface. In addition, the brittle nature of the fashion becomes a source of hydrogen diffusion in the high-tensile strength steel before it concentrates, causing intensified tensile stress at the affected location. Moreover, the simplification adopted in this study includes the type of test used to assess the material's susceptibility to failure. In this instance, the tensile, hardness, impact, surface morphology test are featured to examine the material failure.

4. 2. The damage condition

In this work, the investigation covers the chemical composition test, hardness test, tensile test, impact test, macro and microstructure test, crack surface analysis test. The API 5DP G105 was provided to study the effect of hydrogen embrittlement on the high-strength steel materials (Fig. 1).

Based on the field report, the material was subjected to a pressure of 10.000 psi to assess the drilling resistance, as simulated with a pressure equivalent to 10.000 psi. In this stage of well completion, HDCF injection was performed. To investigate a specific drill pipe failure, the as-received material was delivered to a laboratory to determine the root cause. The damage mechanisms of each drill pipe were examined via visual inspection. Based on the above condition, the presence of longitudinal cracks, pitting, and the presence of fracture location is given. However, the effect of pressure is critical to consider in conjunction with the probability of material to experience local or global crack (Table 1).

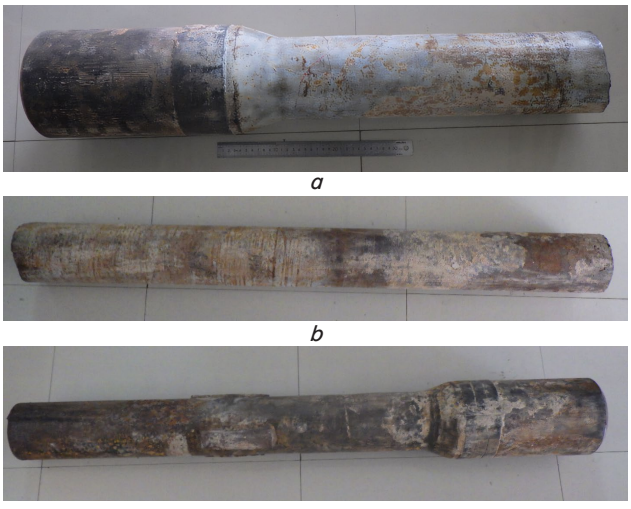

a

b

c

Fig. 1. The as-received drill pipe material:
a – drill pipe A; *b* – drill pipe B; *c* – drill pipe C

Table 1

The failed pipe data based on the actual condition

Parameter	Value
Outer diameter (inch)	5
Thickness (inch)	0.362
Internal diameter (inch)	4.638
Total surface area of drill pipe (inch^2)	3.014

Table 1 differentiates the drill pipe parameters by actual dimensions, allowing the load pressure to be validated. In addition, the pressure test of the TCP and DST BHA from the surface to 2,819 ft MD was performed, with no indication of any defect. The pressure test was deepened to 8,031 ft MD with the same pressure of 10,000 psi before the installation of BPV, TIH, and DST was made from 8023 to 8,059 ft MD, and the running tools of the 13-5/8″ BOP were released. at the same pressure of 10,000 psi. The set packer installation was performed in a counterclockwise manner with TDS. During the BHA retrieval at a depth of 8061 feet, a crack was observed in a slip area approximately 80 cm from the tool joint box. The details of the acronym are provided in Table 2.

Based on the field report, the mud properties indicate a high chloride content of 2000 mg/L, a pH of 9.2, and a molecular weight of 13.1 ppg. The inspected wall thickness of the failed material was 0,357 inch. Fig. 2 shows the crack condition of fractured drill pipe upon retrieval of the

Table 2

The acronym lists

Acronym	Remarks
TCP	Tubing conveyed perforation
DST	Drill stem test
BHA	Bottom-hole assembly
BPV	Back pressure valve
TIH	Trip in hole
TDS	Top drive system
BOP	Blowout preventer
PPG	Pounds per gallon

Fig. 2. The crack location of the fractured drill pipe

It is clear that the corroded steel pipe exhibits circumferential crack where the crack is perpendicular to axial stress (Fig. 2). In this work, the sample A and B were delivered to lab to obtain several tests such as impact, tensile, optical emission spectroscopy (OES), hardness, scanning electronic microscope-energy dispersive X-ray spectroscopy, and microstructure (metallography), where the location is depicted in Fig. 3.

Fig. 3, *a*, *b* show various locations of types of tests according to the damage of failed material and the possible location of hydrogen impact that lowers the mechanical properties of the drill pipe.

Furthermore, each of the samples was prepared to provide specific sample code A, B, and C as illustrated in Fig. 4.

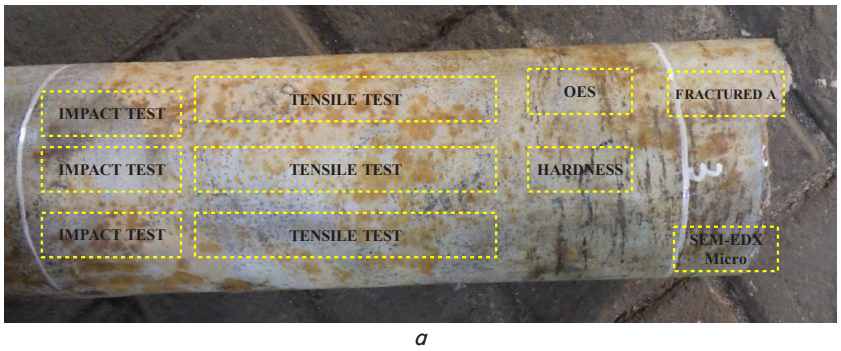

a

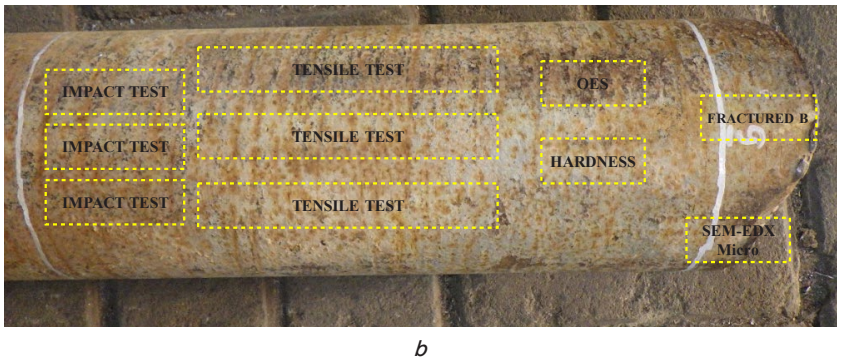

b

Fig. 3. The proposed location for the test and examination:
a — fractured sample A; *b* — fractured sample B

a

b

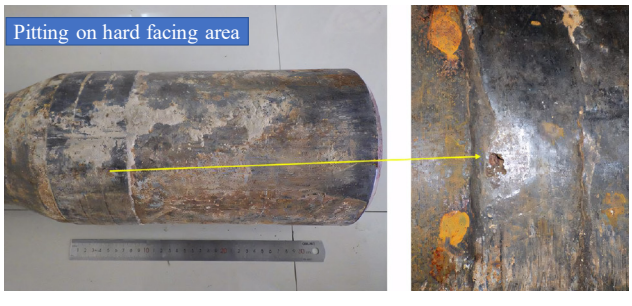

c

Fig. 4. The testing specimen:
a — drill pipe A (fracture A); *b* — drill pipe B (fracture B);
c — drill pipe C (fracture C)

Fig. 4 presents a designated test specimen for each drill pipe. In this study, the drill pipe specimen exhibits notable material degradation, including die marks, pitting, and localized rust. The specimen was subjected to mechanical property assessments and surface characterization.

4. 3. Completion fluid analysis

The chemical test was conducted using optical emission spectrometry (OES) by utilizing Bruker® Q4POLO that adheres to the ASTM A 751 and ASTM E 415. The specimen was prepared from a drill pipe to achieve the dimensions of 3 cm × 3 cm × 1 cm. Three types of completion fluid were examined, including the fresh HDCF fluid, spent HDCF fluid (brine water and HDCF) from the well, and the brine mud (Fig. 5).

The HDCF fluid from various locations is retrieved to compare the effects of impurities on the mechanical properties of drill pipe. The presence of impurities such as chloride, bicarbonate, and carbonate from fluid sample was analyze to delve into susceptibility of API 5DP material against embrittlement (Fig. 5).

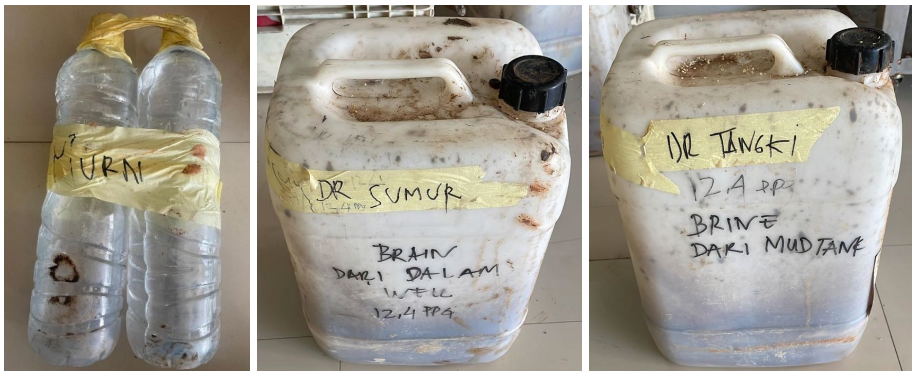

a *b* *c*

Fig. 5. High-density completion fluid sample at various locations: *a* — fresh; *b* — Spent fluid from the well; *c* — brine mud fluid

4. 4. Tensile and hardness test

Understanding the root cause of failed material, particularly in terms of hydrogen embrittlement material susceptibility, is critical. The process began by preparing a sample of drill pipe to a dimension of 3 × 3 × 1 cm. Using the Rockwell Hardness Tester of Rocky D-150 (Fig. 6), the prepared sample underwent examination by adhering to ASTM E18.

Fig. 6. The hardness testing machine

The tensile test was carried out using a Shimadzu Servopulser Universal Tensile Machine according to ASTM E8. The specimen was cut from the sample of drill pipe from the longitudinal direction before being machined into a dog-bone specimen (Fig. 6).

4. 5. Impact test

The impact test was intended to evaluate the drill pipe toughness based on ASTM E23. Three specimens of the impact test specimen was simulated to using GoTech Charpy Impact Tester (GT-7052). The specimen was prepared in the longitudinal direction with a length of 55 mm, a surface area of 10 × 10 mm, and a depth of 2 mm in the mid-section of the specimen.

4. 6. Metallography, macro and micro test

The metallography test was utilized to observed the micro-structure of the failed drill pipe from fracture A and B sample as depicted in Fig. 7, *a*, *b*. The preparation of the specimen was adhered to ASTM E3 through mounting, grinding, polishing, and etching with Nithal 2% solution.

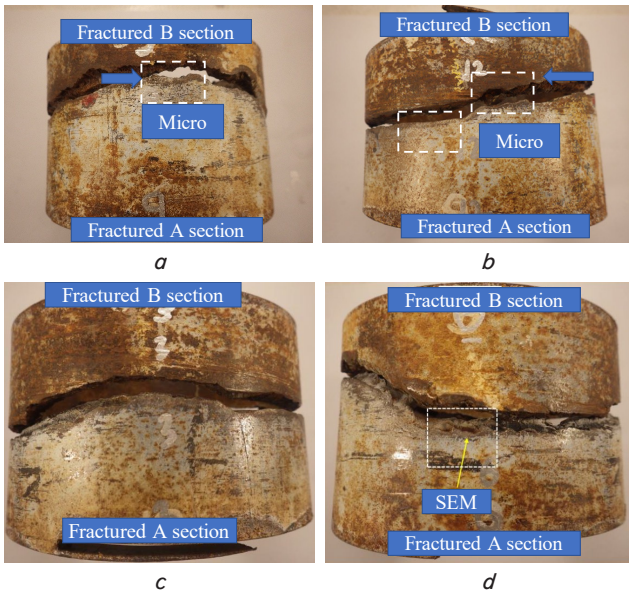

a *b* *c* *d*

Fig. 7. The micro and macro test location: *a* — 9 o'clock; *b* — 12-o'clock; *c* — 3-o'clock; *d* — 6 o'clock

The macro test was made on the specimen according to ASTM E340 while the micro test was subject to ASTM E407 to delve into the thinning susceptibility and the crack propagation on the cross-section (Fig. 7).

4. 7. Surface morphology characterization

The surface characterization was implemented to highlight of the failure mechanism and reveal the contributing factors of failure at the microscopic and level in the proximity of the crack level (Fig. 3). The specimen was prepared from the edge of fractured drill pipe using a JEOL JSTM-IT500 equipped with X-ray spectroscopy. The material was prepared from fracture locations A and B to observe the hydrogen embrittlement that has been predicted. The specimen preparation includes preparing a 1 × 1 cm test coupon from locations A and B. In this case, the accelerating voltage of 20 kB with a high-vacuum chamber was utilized by implementing a scanning rate and step size at 20 seconds per frame and 50 nm per step.

5. Results of unveiling the root cause of failure of drill pipe API 5DP material drill pipe failure

5. 1. Chemical composition test

Table 3 shows the laboratory analysis of the HDCF fluid well completion from three locations.

Table 3

The chemical composition result of the well fluid

Parameter	Unit	Sample source		
		Fresh HDCF	Spent HDCF well	Brine mud HDCF fluid
pH	N/A	9.06	8.91	9.03
SG	lb/gal	13.6	12.5	12.4
TDS	ppm	350,400	465,800	466,400
Fluoride (F^-)	ppm	81	73	68
Chloride (Cl^-)	ppm	1000	900	800
Bicarbonate (HCO_3^-)	ppm	89.79	129.33	140.46
Carbonate	ppm	88.32	127.21	138.16
Bisulfide (HS^-)	ppm	≤ 50	≤ 50	≤ 50
Sulfide (S^{2-})	ppm	≤ 50	≤ 50	≤ 50

Overall, the pH of the three samples indicates an alkaline system, with the spent HDCF notably exhibiting a lower pH of 8.91 compared to the other solutions. The presence of chloride at 900 ppm signifies a moderate concentration that may promote pitting corrosion. Furthermore, the detection of bicarbonate and carbonate ions at 129.33 ppm and 127.21 ppm suggests a moderate level of alkalinity, which can potentially lead to the formation of scale, such as calcium carbonate. Additionally, in the brine mud HDCF fluid system, a chloride content of 800 ppm indicates moderate salinity. The elevated bicarbonate and carbonate levels at 140 ppm and 138 ppm imply a more alkaline, buffered system. It is hypothesized that ions such as chloride, bicarbonate, and carbonate influence hydrogen generation and absorption into steel.

On the other hand, Table 4 shows the result of chemical composition using optical emission spectroscopy (OES), which was verified from three specimens A-C.

Table 4

The chemical composition of drill pipe

Sample code	Element (%)							
	C	Si	Mn	P	S	Cr	Mo	Fe
A	0.222	0.266	1.12	0.014	0.015	0.97	0.178	97.1
B	0.234	0.266	1.132	0.104	0.015	0.971	0.178	97.08
C	0.213	0.259	1.116	0.013	0.014	0.938	0.164	97.16

The presence of P in specimen B has the highest value of 0.104% compares to the rest of the sample code of A and C and tend to more vulnerable to hydrogen embrittlement. On the other hand, the sulfur content of the entire specimen has a minor to moderate effect to HE. The presence Cr at 0.97% exhibits an indirect effect on HE susceptibility (Table 4).

5. 2. Hardness test result

Table 5 shows the hardness test results of three specimens of drill pipe A to C based on the standard of ASTM E18.

Table 5

The hardness test of drill pipe result

Drill pipe specimen	Hardness (HRC)
A	28
B	28
C	27

It is clear that the range of hardness value of drill pipe A-C spans from 27–28 is typical to the tempered martensitic microstructure. It is true that the hardness of material remains within the acceptable range despite their susceptibility against hydrogen-assisted cracking remains observable (Table 5).

5. 3. Impact and tensile test result

Table 6 showcases the result of Charpy impact test result of three specimen at the room temperature.

Table 6

The impact test result

Sample code	Average absorbed energy (Joule)
A	124
B	122
C	119

It is noteworthy to note that the impact test value of the entire drill pipe A to C remains higher than that of the standard of API 5DP material [17]. Based on the above value, the entire material exhibits strength and toughness due to higher Charpy energy and improvement brittle fracture improvement when exposed to hydrogen environment. Despite a noticeable value of Charpy energy, the fracture observation and analysis and service condition remains critical to validate the root cause of the entire samples.

In addition, Table 7 illustrates the average tensile test result of the specimen to reveal the mechanical properties of failed material.

Table 7

The tensile test results

Sample code	Yield strength (MPa)	Tensile strength (MPa)	Elongation (%)	Standard elongation (%)
Drill pipe A	841	914	21	11
Drill pipe B	827	909	20	11
Drill pipe C	831	908	20	11
Standard API 5DP	730–930	Min 790	Min	NA

Based on Table 7, the majority of specimens adhered to the API 5DP material standard. The highest yield strength (YS), tensile strength (TS), and elongation of drill pipe A are 841 MPa, 914 MPa, and 21%. In this case, the high YS and TS correspond to the primary driver of HE risk and increase their susceptibility. This value is comparable to the finding of [18], the embrittlement was induced by thermomechanical activity within the heat-affected zone (HAZ). Furthermore, the elongation value of 21% indicates that the material retains its ductile characteristics, despite its susceptibility to brittleness during service.

In this instance, it is prime to demonstrate that the presence of the sulfide and bisulfide increase the hydrogen ion concentration in the well fluid through decomposition reaction as depicted in equation (1):

$$H_2S \rightarrow HS^- + H^+,$$

$$HS^- \rightarrow H^+ + S^{2-}. \quad (1)$$

Thus, it is possible to note that the ductility reduction appears as more hydrogen atoms are diffused into materials.

5. 4. Surface characterization result

Fig. 8 illustrates the macro observation result of the fracture specimen A and B to define the fracture morphology of the failed material.

a *b*

Fig. 8. The surface macrophotograph:
a — drill pipe A; *b* — drill pipe B

It is noteworthy to observe that the thickness of the affected fractured material exhibits no thinning on either the outer or inner surface of the pipe. The thickness at the 12 o'clock position remains unchanged, confirming the brittle fracture mechanism. This mechanism is consistent with hydrogen embrittlement, particularly when the material shows no evidence of plastic deformation. The cup-and-cone fracture is observed, which correlates with the higher Charpy impact energy attributable to the greater energy-absorbing capacity of drill pipes A and B (Table 5).

Fig. 9 depicts the information related to the metallography test result of the specimen.

Fig. 9, *a* illustrates a surface-connected crack prior to the appearance of a propagation crack, exhibiting a relatively straightforward crack pathway and minimal branching. Furthermore, the dark, sharply defined crack edges are consistent with the material's brittle nature, which lacks ductile tearing properties [19]. Surface crack initiation begins near the surface and indicates a reduction in ductility as the material propagates inward. Furthermore, the crack morphology reveals a propagation path that aligns with a high tensile strength value [20].

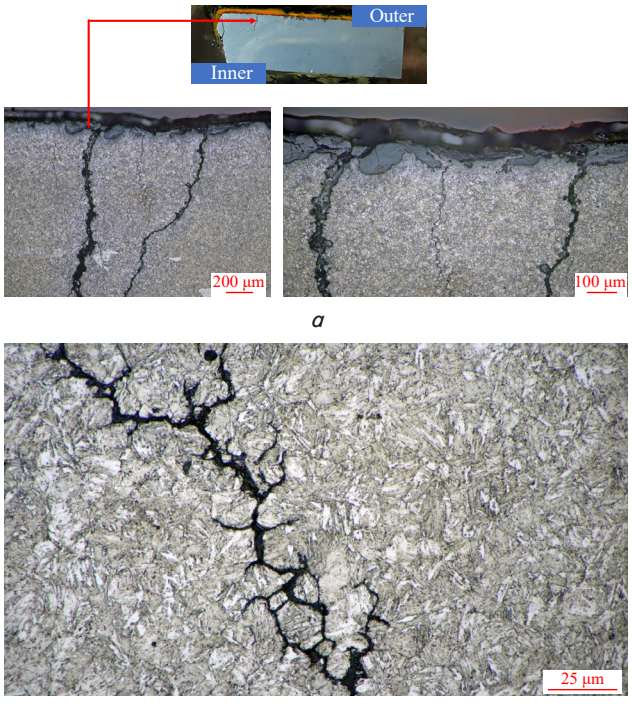

a

b

Fig. 9. The micro-structure photograph of the failed specimen: *a* — cross-section; *b* — crack propagation along austenitic grain boundary

Fig. 9, *b* highlights the presence of highly branched cracks with irregular crack directions. The crack propagation features secondary cracks, which are typically associated with hydrogen embrittlement. However, this result remains consistent with the SEM-EDX analysis to substantiate the metallography findings (Fig. 10).

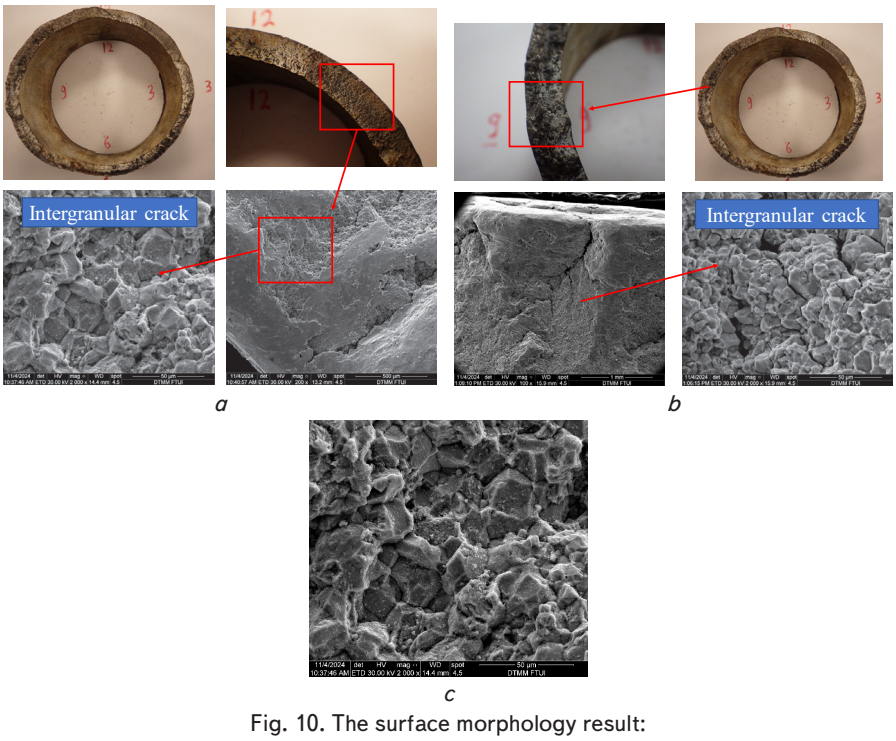

a *b*

c

Fig. 10. The surface morphology result:
a — initiation crack of the fractured surface; *b* — the underneath of fractured location; *c* — rocky-candy intergranular crack

Fig. 10 provisions the scanning electronic microscope of the fracture analysis of the failed drill pipe. It is essential to note that the rocky-candy structure of the API 5DP material adheres to the intergranular fracture. In this case, the SEM result is in good agreement with the metallography findings where the intergranular crack appears on the drill pipe material and propagate on the austenitic grain boundary. The similar observation was aligned with the study [21] in which the material of Fe-Cr-Ni-Mn-Mo-Si-N-C alloys experiences electrochemical hydrogen charged along grain boundaries. In this work, the rocky-candy structure is equivalent as austenite grain of the drill pipe. The intergranular fracture mode is considered a brittle fracture where the alloy exhibits crack propagation on the grain boundary of the material. Hence, it is essential to describe the damage mechanism of the material as illustrated in Fig. 11.

Fig. 11 depicts the drill pipe condition when they simulated during flexing process. During well completion, the drill pipe was hung on the HDCF fluid leads to increase the tension downward, where the density of HDCF is 13.6 lb/gal.

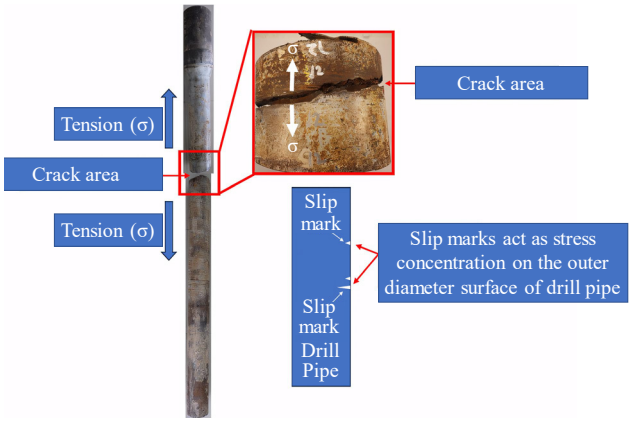

Fig. 11. The illustration of the tension and slip marks as a stress concentration

Based on Fig. 11, the disappearance of deformation on the crack area is evident and aligns with the result of the tensile test. It is also prime to test whether the brittleness appears globally or locally on the crack area by considering the pressure loaded to cause the ductile crack. Based on the data in Table 1, it is concluded that brittleness appears locally in the cracked area rather than globally.

Additionally, the drill pipe exhibited resistance to deformation in the crack area, indicating that its fracture is ductile. This is consistent with the high tensile strength being lower than the ultimate tensile strength. For specimen A, the tensile strength is 914 MPa, which causes a brittle fracture characterized by intergranular cracking (Fig. 9, 10).

6. Discussion of root cause analysis for drill pipe

In this study, the drill pipe failure occurred during well completion when the HDCF was added. According to the report, the drill pipe was used for almost two weeks before failure. Hence, the effects of well fluid and the vulnerability of the crack material are important factors to consider. Table 3 shows the presence of chlorides, bicarbonates, and carbonates elicit the evidence of impurities from the HDCF particularly from the spent HDCF. The ionic species is possibly related to the promotion of the localized corrosion where the penetration of hydrogen atoms can lead to brittle cracking. In this case, the metal dissolution becomes a crack initiation as the primary driver to promote the hydrogen diffusion [22]. The high concentration of chloride ions correlates with the aggressiveness of these ions on the steel surface, leading to the breakdown of the protective films of API 5DP material prior to the onset of steel destabilization, which can result in sustained corrosion. Furthermore, the presence of these ions contributes to oxygen depletion, lowers the pH, and acts as a precursor to hydrogen generation (Table 3). In instances where bicarbonate and carbonate ions originate from the spent HDCF fluid, they are observed to supply hydrogen within the well fluid.

It is critical to discuss that the presence of bisulfide and sulfide ions in the water chemistry testing (Table 3). It is noteworthy to remember that the contamination of brine and H_2S gas during well completion process to allow dissociation of bisulfide (HS^-) and sulfide (S^{2-}). On the other hand, the possible source of H_2S gas is due to the injection of corrosion inhibitor especially from the halide-brines completion fluid [23]. According to the study [24], adding thiocyanate (SCN^-) at high temperature and pressure releases H_2S gas and sulfur, which can poison high-strength steels like API 5DP.

Although hydrogen production diminishes at a higher pH of 8.91, the formation of scale induces under-deposit corrosion. It is noteworthy that a localized corrosion cell is established, facilitating localized attack and causing hydrogen to diffuse and accumulate at specific traps [25].

Table 4 highlights several elements that contribute to the increased susceptibility of API 5DP material to HE. As shown in Table 4, the identification of P at 0.104% in specimen B is considered indicative of the material's resistance to HE, since at higher phosphorus levels, the element appears capable of controlling the grain boundary associated with HE [26]. In this case, phosphorus segregation affects embrittlement and decreases the material's toughness. This results in a slightly lower Charpy impact value of 122 Joules for specimen B compared to specimen A. Moreover, the presence of phosphorus weakens grain-boundary strength by disrupting metallic bonds and reducing grain cohesion. Consequently, atomic hydrogen can more easily penetrate and enter the grain boundaries.

This phenomenon indicates the material's increased hardness and aligns with the hardness results for specimens A-C (Table 5). Specifically, the hardness of drill pipe specimens A and B is 28, while that of C is 27, highlighting the critical threshold for HE vulnerability. With this in mind, the HE susceptibility appears when the grain boundary is weakened and allow the hydrogen dissipation to weak the boundaries. With the exposure of drill pipe in mud during well completion at more than two week allows the corrodents such as chloride, carbonates, and sulfides to further corrodent on the surface of API 5DP. Also, the corrosive environment during well completion generates hydrogen and accelerates crack growth in the material [27]. However, this single experiment remains insufficient to completely capture the HE phenomenon.

Table 6 illustrates the resistance of each test specimen against early brittle failure when API 5DP drill pipe is in service during well completion. Simultaneously, the values of tensile strength and yield strength of drill pipe A–C appear to exceed the standard API 5DP specifications. Drill pipe A exhibits the highest tensile strength at 841 MPa, indicating susceptibility to hydrogen embrittlement (HE), despite a notable elongation of 22% and a moderate Charpy impact energy of 124 Joules.

Conversely, the specimen drill pipe C demonstrates resistance of the API 5DP material against HE. Its yield strength, tensile strength, and elongation are 831 MPa, 908 MPa, and 20%, respectively, which are associated with a decrease in crack propagation resistance despite prolonged exposure to a corrosive environment, thereby rendering the material susceptible to degradation [28]. The data remains consistent with actual conditions, where slip marks were observable as stress concentrators on the failed material (Fig. 11).

During well completion, the drill pipe was hung on the HDCF fluid leads to increase the tension downward. The HDCF density is 13.6 lb/gal. Additionally, the drill pipe showed resistance to deformation in the crack area, indicating that its fracture is ductile in nature. This is consistent with the high tensile strength being lower than the ultimate tensile strength. For specimen A, the tensile strength is 914 MPa, which causes a brittle fracture characterized by intergranular cracking (Fig. 9, 10). Furthermore, the observed higher elongation aligns with ductile behavior and confirms that there is no significant shift from ductile to brittle failure [29].

Fig. 8 shows the macro-observation of two specimens of the fracture specimen and to show the features of hydrogen assisted fracture. Based on Fig. 8 *a*, the rough and granular outer region appear to show the irregular while faceted edge surface although the surface shows a cup-and-cone of ductile fracture [30]. In consonance, the presence of rocky texture becomes more apparent to show the intergranular fracture and consistent with the result of surface characterization (Fig. 10, *a*, *b*).

Moreover, the metallography results show the presence of tempered martensite and to confirm that the drill pipe material has been quenched and tempered during manufacturing process. In this case, the quenching and tempering become precursor to improve the strength of the alloy.

Based on Fig. 9, the outer surface of the pipe (OD) exhibits numerous shallow depressions, which are suspected to be traces of slip marks and pitting. Cracks are frequently observed initiating from these stress concentrations. These cracks propagate extensively from the outer surface toward the inner surface of the pipe and display a branched morphology. Observations at 500× magnification (Fig. 9) reveal that the cracks propagate along the austenite grain boundaries, forming small island-like features. It is also possible to note that the martensitic structure renders it more prone to HE as high-density of dislocations is produced [31]. A high concentration of hydrogen enables the crack to grow along the grain boundary, resulting in intergranular fracture. It is also possible to note that the crack propagate inward to indicate the hydrogen diffused inward due to stress during flexing activity and the martensitic microstructure.

Fig. 10 confirms the result of metallography where the intergranular crack on the drill pipe remains propagate on the grain boundary austenite. The rocky-candy structure enhances the visibility and length of slip marks and describe the grain boundary deformation. This behavior related to the crack initiation and hydrogen embrittlement behavior. The presence of slip marks on the outer diameter of failed material behaves as a stress concentrator and serves as initiation crack. This fracture is worsen when the API 5DP material is exposed with the HDCF material. As illustrated in equation (1), the hydrogen ions in the brine well fluid adsorb onto the surface of API 5DP material, enhancing its embrittlement. Because of their extremely small atomic size, hydrogen atoms can diffuse into the solid metal lattice. Once absorbed, hydrogen lowers the stress needed for crack initiation and growth, markedly increasing the risk of brittle failure.

On top of it, this work requires complimentary tests such as slow strain rate testing as the hydrogen embrittlement appearance requires time to occur. This fact becomes a disadvantage of the study due to a loss of ductility due to hydrogen penetration requires time even at minor hydrogen concentrations to observe the initiation and propagation crack growth. Moreover, the existing testing remains difficult to replicate the actual or in-service of drill pipe conditions. A gradual fluctuation in pressure exposing to the drill pipe and the existing H_2S with consideration of residual stress are a few critical factors to consider whether the existing study is aligned to the actual in-service of drill pipe.

The limitation of this study is given on the absence of hydrogen content measurement. In this case, due to small and mobile hydrogen atoms, it limits the how to include the effect of hydrogen concentration on the specimen and the distribution of hydrogen during testing. It leads to difficulty to provide accurate hydrogen concentration on the stress concentrator area and makes measurement becomes challenging. Therefore, it is common to utilize the thermal desorption analysis to obtain the electrochemical permeation of hydrogen diffusion to track the increase of hydrogen concentration as the crack initiates and propagates. Moreover, this study can be further developed into a slow strain rate tensile test (SSRT) to evaluate the relative change in mechanical properties with or without hydrogen, considering variations in the test specimen temperature. Thus, future studies would demonstrate the hydrogen embrittlement mechanism by mapping microstructure and conducting a comprehensive root cause analysis.

7. Conclusions

1. The spent HDCF well fluid contains significant concentrations of chloride, bicarbonate, and carbonate ions, which are associated with the corrosion process and induce localized corrosion prior to the ingress of hydrogen atoms into the metallic surface of API 5DP. The presence of phosphorus identified in specimen test B indicates reduced cohesive bonds and grain-boundary segregation, thereby weakening metallic bonding and facilitating hydrogen diffusion.

2. The magnitude of the hardness value, which ranges from 27–28 HRC, retains the susceptibility of API 5DP material against HE. Therefore, the high hardness value reduces the material's resistance to HE.

3. The Charpy impact energy, tensile strength, yield strength show an embrittlement behavior. The brittle behavior appears locally, which is located only in the fractured area due to the weakened grain boundary of the material.

4. The macro structure conforms to the micro-structure outcome, where the presence of hydrogen diffusion leads to embrittlement at the surface void and dislocation due to corrosion. The corrosive species such as chloride, bicarbonate, carbonate, bisulfide and sulfide increase the number of active sites for the hydrogen atom diffusion.

Conflict of interest

The authors declare that they have no conflict of interest in relation to this study, whether financial, personal, authorship

or otherwise, that could affect the study and its results presented in this paper.

Financing

The study was performed without financial support.

Data availability

Data cannot be made available for reasons disclosed in the data availability statement.

Use of artificial intelligence

The authors confirm that they did not use artificial intelligence technologies in creating the submitted work.

Authors' contributions

Sidhi Aribowo: Writing – Original Draft, Visualization, Formal analysis, Investigation, Data Curation, Methodology; **Johny Soedarsono**: Conceptualization, Supervision, Methodology, Formal Analysis; **Rini Riastuti**: Supervision, Validation, Conceptualization, Resources, Methodology, Formal Analysis; **Suryadi**: Investigation, Methodology, Formal Analysis, Validation; **Slamet Nurhadi**: Investigation, Resources, Methodology, Formal Analysis, Validation; **Warneri**: Investigation, Conceptualization, Resources, Methodology, Formal Analysis, Validation; **Sopar Mangarapot Simanullang**: Investigation, Resources, Methodology, Formal Analysis, Validation; **Agus Paul Setiawan Kaban**: Data curation, Visualization, Formal analysis, Validation; **Raajwa Ayudhia Kamila**: Writing – Review & Editing, Visualization, Formal analysis, Investigation, Funding acquisition.

References

1. Laureys, A., Depraetere, R., Cauwels, M., Depover, T., Hertelé, S., Verbeken, K. (2022). Use of existing steel pipeline infrastructure for gaseous hydrogen storage and transport: A review of factors affecting hydrogen induced degradation. Journal of Natural Gas Science and Engineering, 101, 104534. https://doi.org/10.1016/j.jngse.2022.104534
2. Aditiyawarman, T., Soedarsono, J. W., Kaban, A. P. S., Riastuti, R., Rahmadani, H. (2022). The Study of Artificial Intelligent in Risk-Based Inspection Assessment and Screening: A Study Case of Inline Inspection. ASCE-ASME Journal of Risk and Uncertainty in Engineering Systems, Part B: Mechanical Engineering, 9 (1). https://doi.org/10.1115/1.4054969
3. Sridharan, V. S., Verma, V. K., Narayan, R. L., Lu, X., Siwei, D., Chaudhary, V. et al. (2025). Hydrogen embrittlement of additively manufactured metallic materials. International Journal of Hydrogen Energy, 121, 245–272. https://doi.org/10.1016/j.ijhydene.2025.03.222
4. Mokhtari, E., Heidarpour, A., Javidan, F. (2024). Mechanical performance of high strength steel under corrosion: A review study. Journal of Constructional Steel Research, 220, 108840. https://doi.org/10.1016/j.jcsr.2024.108840
5. Oriani, R. A. (1972). A mechanistic theory of hydrogen embrittlement of steels. Berichte Der Bunsengesellschaft Für Physikalische Chemie, 76 (8), 848–857. Portico. https://doi.org/10.1002/bbpc.19720760864
6. Damage Mechanisms Affecting fixed Equipment in the Refining Industry (2003). Recommended Practice 571 First Edition. API.
7. Wu, X., Song, Z., Tan, M., Jia, W., Liu, J. (2026). Hydrogen-induced failure mechanism of X80 pipeline steel welded joints based on macro-and micro-scale experimental analysis: Embrittlement enhancement effect caused by high hydrogen trap density. Engineering Failure Analysis, 183, 110190. https://doi.org/10.1016/j.engfailanal.2025.110190
8. Zekun, Y., Zhanli, Y., Hao, Y., Yan, Z., Kai, X. (2025). Hydrogen embrittlement in welded joints of high-strength pipeline steels: A review of mechanisms, characterization, and mitigation strategies. International Journal of Pressure Vessels and Piping, 218, 105615. https://doi.org/10.1016/j.ijpvp.2025.105615
9. Kawamori, M., Shibata, K., Yoda, R., Morita, S., Fujita, Y., Kuroda, S. et al. (2025). Dual effects of deformation on hydrogen embrittlement of austenitic stainless steels revealed by hydrogen visualization combined with microstructural analysis. International Journal of Hydrogen Energy, 145, 559–577. https://doi.org/10.1016/j.ijhydene.2025.05.426
10. Kawamori, M., Yuse, F. (2023). In-situ measurement of hydrogen entry and hydrogen embrittlement of steel by atmospheric corrosion. Corrosion Science, 219, 111212. https://doi.org/10.1016/j.corsci.2023.111212
11. Lan, X., Okada, K., Ueji, R., Shibata, A. (2025). Improving hydrogen embrittlement resistance in high-strength martensitic steels via thermomechanical processing. Scripta Materialia, 264, 116711. https://doi.org/10.1016/j.scriptamat.2025.116711
12. Hwang, Y., Park, H., Yun, H. S., Bae, K.-O., Baek, U. B., Lee, J. (2025). Effects of sensitization on hydrogen embrittlement behavior in 304 stainless steel. Materials & Design, 260, 115130. https://doi.org/10.1016/j.matdes.2025.115130
13. Dong, X., Wang, D., Thoudden-Sukumar, P., Tehranchi, A., Ponge, D., Sun, B., Raabe, D. (2022). Hydrogen-associated decohesion and localized plasticity in a high-Mn and high-Al two-phase lightweight steel. Acta Materialia, 239, 118296. https://doi.org/10.1016/j.actamat.2022.118296
14. Asadipoor, M., Pourkamali Anaraki, A., Kadkhodapour, J., Sharifi, S. M. H., Barnoush, A. (2020). Macro- and microscale investigations of hydrogen embrittlement in X70 pipeline steel by in-situ and ex-situ hydrogen charging tensile tests and in-situ electrochemical micro-cantilever bending test. Materials Science and Engineering: A, 772, 138762. https://doi.org/10.1016/j.msea.2019.138762
15. Singh, R., Sharma, R., Rao, G. R. (2023). A comprehensive review on the high-density clear completion fluids for applications in HPHT well completion. International Journal of Oil, Gas and Coal Technology, 32 (1), 70. https://doi.org/10.1504/ijogct.2023.127337
16. Peng, X., Yu, H., Lian, Z., Dong, B., Zhong, W., Zhang, Y., Hu, Z. (2021). Material optimization of drill pipe in complex wellbore environments by comparing fatigue life and cost. Energy Reports, 7, 5420–5430. https://doi.org/10.1016/j.egyr.2021.08.135

17. Zamani, S. M., Hassanzadeh-Tabrizi, S. A., Sharifi, H. (2016). Failure analysis of drill pipe: A review. Engineering Failure Analysis, 59, 605–623. https://doi.org/10.1016/j.engfailanal.2015.10.012
18. Atamashkin, A., Priymak, E., Tulibaev, E., Syomka, Y., Trushov, V. (2024). Influence of force parameters of rotary friction welding on the microstructure and mechanical properties of welded joints of high-strength drill pipes. International Journal on Interactive Design and Manufacturing, 19 (4), 2937–2950. https://doi.org/10.1007/s12008-024-02011-w
19. Cho, L., Bradley, P. E., Lauria, D. S., Connolly, M. J., Seo, E. J., Findley, K. O. et al. (2021). Effects of hydrogen pressure and prior austenite grain size on the hydrogen embrittlement characteristics of a press-hardened martensitic steel. International Journal of Hydrogen Energy, 46 (47), 24425–24439. https://doi.org/10.1016/j.ijhydene.2021.05.005
20. Yu, H., He, J., Morin, D. D., Ortiz, M., Zhang, Z. (2025). A self-consistent void-based rationale for hydrogen embrittlement. Scripta Materialia, 255, 116403. https://doi.org/10.1016/j.scriptamat.2024.116403
21. Kim, K.-S., Kang, J.-H., Kim, S.-J. (2019). Effect of Grain Boundary Carbide on Hydrogen Embrittlement in Stable Austenitic Stainless Steels. ISIJ International, 59 (6), 1136–1144. https://doi.org/10.2355/isijinternational.isijint-2018-639
22. Puiggali, M., Zielinski, A., Olive, J. M., Renauld, E., Desjardins, D., Cid, M. (1998). Effect of microstructure on stress corrosion cracking of an Al-Zn-Mg-Cu alloy. Corrosion Science, 40 (4-5), 805–819. https://doi.org/10.1016/s0010-938x(98)00002-x
23. Howard, S., Chrenowski, M. (2014). Corrosion in Formate Brines – 20 Years of Laboratory Testing and Field Experience. Offshore Technology Conference-Asia. https://doi.org/10.4043/24983-ms
24. Silverman, S. A., Bhavsar, R., Edwards, C., Virally, S., Foxenberg, W. (2003). Use of High-Strength Alloys and Elastomers in Heavy Completion Brines. SPE Annual Technical Conference and Exhibition. https://doi.org/10.2118/84515-ms
25. Espinosa-Medina, M. A., la Torre, G. C.-D., Castillo, A. S., Ángeles-Chávez, C., Zeferino-Rodríguez, T., González-Rodríguez, J. G. (2017). Effect of Chloride and Sulfate Ions on the SCC of API-X70 Pipeline Welds in Diluted Carbonated Solutions. International Journal of Electrochemical Science, 12 (8), 6952–6965. https://doi.org/10.20964/2017.08.07
26. Komazazki, S.-I., Watanabe, S., Misawa, T. (2003). Influence of Phosphorus and Boron on Hydrogen Embrittlement Susceptibility of High Strength Low Alloy Steel. ISIJ International, 43 (11), 1851–1857. https://doi.org/10.2355/isijinternational.43.1851
27. Nanninga, N., Grochowsi, J., Heldt, L., Rundman, K. (2010). Role of microstructure, composition and hardness in resisting hydrogen embrittlement of fastener grade steels. Corrosion Science, 52 (4), 1237–1246. https://doi.org/10.1016/j.corsci.2009.12.020
28. Park, H., Yoo, J., Lee, J.-J., Kang, Y., Seo, K. M., Lee, C.-H. et al. (2024). Impact of hydrogen embrittlement on the tensile-shear property of resistance spot-welded advanced high-strength martensitic steels. International Journal of Hydrogen Energy, 71, 319–333. https://doi.org/10.1016/j.ijhydene.2024.05.138
29. Li, X., Zhang, J., Cui, Y., Djukic, M. B., Feng, H., Wang, Y. (2024). Review of the hydrogen embrittlement and interactions between hydrogen and microstructural interfaces in metallic alloys: Grain boundary, twin boundary, and nano-precipitate. International Journal of Hydrogen Energy, 72, 74–109. https://doi.org/10.1016/j.ijhydene.2024.05.257
30. Cui, D., Bai, Y., Xiong, L., Yu, B., Wei, B., Sun, C. (2024). Effects of hydrogen blending ratios and CO2 on hydrogen embrittlement of X65 steel in high-pressure offshore hydrogen-blended natural gas pipelines. Journal of Materials Research and Technology, 33, 4763–4771. https://doi.org/10.1016/j.jmrt.2024.10.150
31. Tong, Z., Wang, H., Zheng, W., Zhou, H. (2024). Change in Hydrogen Trapping Characteristics and Influence on Hydrogen Embrittlement Sensitivity in a Medium-Carbon, High-Strength Steel: The Effects of Heat Treatments. Materials, 17 (8), 1854. https://doi.org/10.3390/ma17081854